ASTROBIOLOGY
Volume 9, Number 7, 2009

DOI: 10.1089/ast.2009.0351

Research Article

Laser-Induced Fluorescence Emission (L.I.F.E.): *In Situ* Nondestructive Detection of Microbial Life in the Ice Covers of Antarctic Lakes

Michael C. Storrie-Lombardi[1] and Birgit Sattler[2]

Abstract

Laser-induced fluorescence emission (L.I.F.E.) images were obtained *in situ* following 532 nm excitation of cryoconite assemblages in the ice covers of annual and perennially frozen Antarctic lakes during the 2008 Tawani International Expedition to Schirmacher Oasis and Lake Untersee in Dronning Maud Land, Antarctica. Laser targeting of a single millimeter-scale cryoconite results in multiple neighboring excitation events secondary to ice/air interface reflection and refraction in the bubbles surrounding the primary target. Laser excitation at 532 nm of cyanobacteria-dominated assemblages produced red and infrared autofluorescence activity attributed to the presence of phycoerythrin photosynthetic pigments. The method avoids destruction of individual target organisms and does not require the disruption of either the structure of the microbial community or the surrounding ice matrix. L.I.F.E. survey strategies described may be of interest for orbital monitoring of photosynthetic primary productivity in polar and alpine glaciers, ice sheets, snow, and lake ice of Earth's cryosphere. The findings open up the possibility of searching from either a rover or from orbit for signs of life in the polar regions of Mars and the frozen regions of exoplanets in neighboring star systems. Key Words: Cryosphere—Ice—Mars—Photosynthesis—Psychrophiles. Astrobiology 9, 659–672.

Introduction

The ices of Earth's polar regions and high mountains, once seen as sterile, harsh environments too poor in nutrients and liquid water to sustain life, are now known to harbor rich, complex microbial communities in the ice ecosystems of alpine and polar lakes, sea ice, glacier ice, and even the ice of supercooled cloud droplets (Priscu *et al.,* 1998; Psenner and Sattler, 1998; Psenner *et al.,* 1999; Sattler *et al.,* 2001, 2004; Priscu and Christner, 2004). Central to the establishment of microbial communities in polar ice is the eolian transport and deposition of dust particles that contain both humic material and microbial life, including photosynthetic cyanobacteria (Psenner, 1999; Porazinska *et al.,* 2004). Dust grains that contain high concentrations of humic material are rich in organic molecules and have a high coefficient of friction, which increases the likelihood that an assemblage will adhere to the ice surface. The darker coloration of such dust grains allows for efficient absorption of solar energy (Takeuchi *et al.,* 2001; Takeuchi and Li, 2008). The resultant local temperature elevation melts the ice beneath the assemblage and forms a cylindrical depression, into which the debris sinks. The descending assemblage is then covered by a new icy surface as the surficial portion of the melt freezes, which produces extreme changes in hydrophysical and hydrochemical conditions for the entrapped microorganisms (Tranter *et al.,* 2004). When ice is in contact with mineral surfaces, a microfilm of water forms around the particle, which can provide liquid water and nutrients to the microbial community (Priscu *et al.,* 1998; Price, 2007).

In the clear ice coverings of Lake Untersee (Fig. 1) and the lakes of the Dry Valleys of Schirmacher Oasis (Fig. 2A), the process is ongoing, given that sunlight penetrates deep into the ice and the solar heated dust continues to melt surrounding ice, such that both the grains and microorganisms remain coated with a thin layer of water. The combination of dust, water, organic matter, sunlight, and life results in a tiny microcosm that derives liquid water and usable energy from the Sun. These accumulations were first called cryoconites (from the Greek kryos, "icy cold," and konia, "dust") by the Swedish explorer A.E. Nordenskjöld during an expedition to the glaciers of Greenland in 1870 (Miteva, 2008). Cryoconite assemblages range in scale from massive boulders, which have melted slowly into Antarctic lakes (Fig. 2B), to small

[1]Kinohi Institute, Pasadena, California.
[2]University of Innsbruck, Institute of Ecology, Innsbruck, Austria.

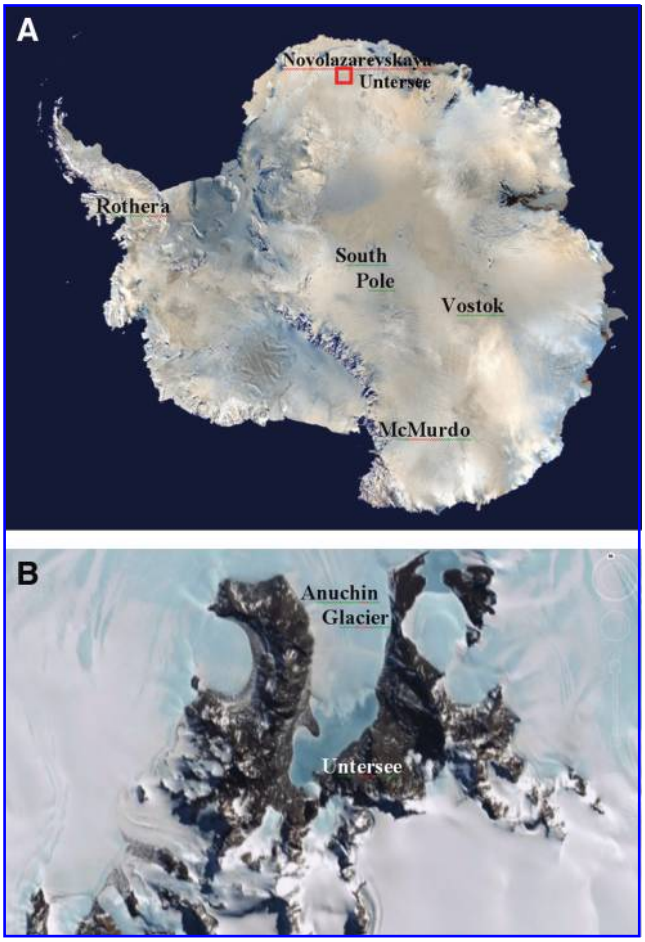

FIG. 1. The Russian support station of Novolazarevskaya (**A**) is situated on the edge of the Schirmacher Oasis, a dry valley within 75 km of the coast and 90 km northwest of the Anuchin Glacier and Lake Untersee (**B**). Color images available online at www.liebertonline.com/ast.

grains in ice that range from a few millimeters to micrometers in diameter (Fig. 2C, 2E). The microbial consortiums that survive in these habitats are dominated by photosynthetic species, particularly cyanobacteria, which play a crucial role in polar aquatic ecosystems (Säwström *et al.,* 2002; Anesio *et al.,* 2009) for primary productivity and biogeochemical cycling (Tranter *et al.,* 2004; Hodson *et al.,* 2005; Foreman *et al.,* 2007; Hodson *et al.,* 2008).

The fragility of the life-forms living in ice, along with the extreme environment they inhabit, has made studying these cryosphere ecosystems difficult. Until now, solid ice had to be disrupted to investigate such microbial communities. Techniques that include coring (Fig. 2D, 2E), sawing, and subsequent melting induce extensive chemical and physical changes in the organisms and their environment. Due to the sensitivity of psychrophiles to even moderate changes in temperature, the need for an *in situ* non-invasive, nondestructive method to detect, localize, and monitor biomass distribution within the cryosphere is of considerable importance.

Laser-induced fluorescence emission (L.I.F.E.) from specific biomolecular intracellular and extracellular targets is arguably the single most sensitive active photonic probe that does not require sample preparation, sample destruction, or limited consumable resources other than power (Asher, 1993). L.I.F.E. biosignatures may be extracted from spectra or images, or identified by combining both data acquisition modes in nonlinear artificial neural networks (Storrie-Lombardi *et al.,* 1992; Lahav *et al.,* 1995). High-resolution epifluorescence microscopy with broadband excitation wavelengths at 254 and 375 nm, and laser excitation of 532 and 660 nm, is standard equipment for aquatic microbiologists. Laser wavelengths between 220 and 250 nm (deep ultraviolet) can excite nucleic acids and aromatic amino acids to produce fluorescence at 300–350 nm, which can be easily detected by an ultraviolet-sensitive camera (Nealson *et al.,* 2002) or spectrometer (Bhartia *et al.,* 2008). The technique applied at these wavelengths has been proposed as a method to search for life on Mars (Storrie-Lombardi *et al.,* 2001). It has also been used on Earth to find microbial life in basal cores 1.3 km below Mauna Kea (Fisk *et al.,* 2003), detect microbial life deep in glacial ice (Price, 2007), and estimate biomass in Greenland ice cores (Rohde *et al.,* 2008). Excitation of critical metabolites found in all living organisms (such as flavin adenine dinucleotide and nicotinamide adenine dinucleotide) with a 375 nm laser evokes fluorescence in the blue and green portion of the visible spectrum (Storrie-Lombardi, 2005) and has been identified as a technique applicable to the European Space Agency's ExoMars mission to search for organic material such as infall polycyclic aromatic hydrocarbons sequestered within the martian regolith (Griffiths *et al.,* 2008; Storrie-Lombardi *et al.,* 2008a; Storrie-Lombardi *et al.,* 2008b). Excitation between 450 and 650 nm produces a fluorescence response in multiple pigments of crucial importance in microbial photosynthesis with characteristic fluorescence signatures appearing between 500 and 800 nm (Blinks, 1954). Photopigments of significance to this work include the phycobiliproteins and the chlorophylls. Phycobiliproteins are found primarily in red algae, cyanobacteria, and cryptomonads, including species that inhabit such extreme environments as ice-covered Antarctic lakes and acidic high-temperature hydrothermal vents. Red algae and cyanobacteria may have all three types of biliprotein: phycoerythrin, phycocyanin, and allophycocyanin (Samsonoff and MacColl, 2001). Allophycocyanin and phycocyanin have been found in all species isolated to date. Red algae and cyanobacteria also contain chlorophyll *a,* and cryptomonads contain both chlorophyll *a* and *c*. In underwater habitats, light is attenuated and its spectral distribution shifted into the blue-green energies better absorbed by the biliproteins than by chlorophyll *a*. Light absorbed by the biliproteins migrates to chlorophyll and then to the photosynthetic reaction centers for transformation into chemical energy. The most commonly encountered cyanobacteria phycobionts of cryptoendolithic lichens in the high-polar regions of Antarctica—*Chroococcidiopsis* sp., *Gloeocapsa* sp., *Gloeocapsa* sp., and *Gloeocapsa* sp.—all produce significant fluorescence response to excitation between 436 nm (Soret band for chlorophyll) and 550 nm, the region of maximum absorption by phycobiliproteins (Erokhina *et al.,* 2002).

Laser-induced fluorescence emission spectral signatures of ocean and lake phytoplankton via 532 nm lasers have been obtained from airborne platforms such as NASA's Airborne Oceanographic LIDAR (Light Detection and Ranging) since 1979 (Hoge and Swift, 1981). The signatures have most

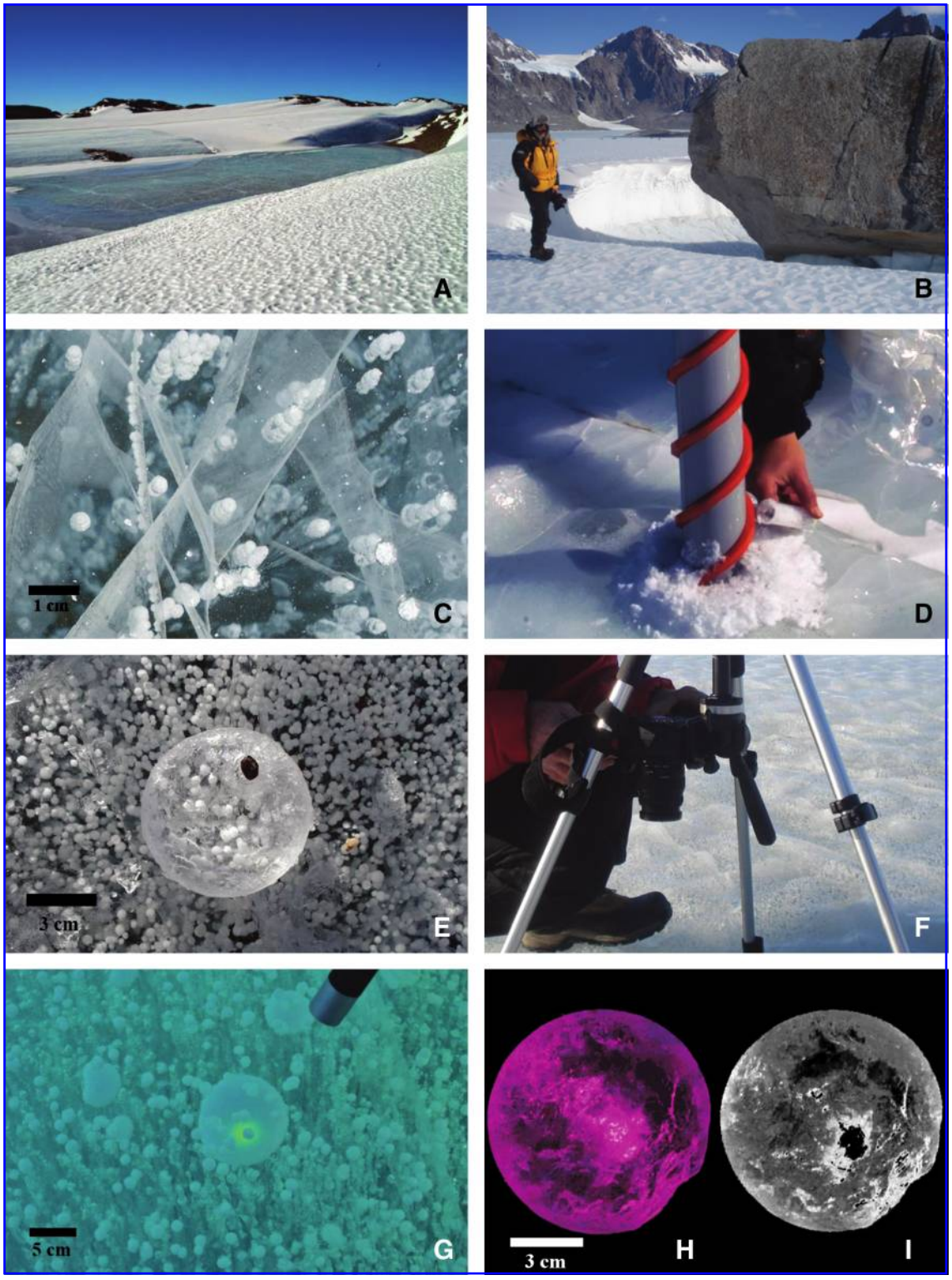

FIG. 2. The Schirmacher Oasis harbors more than 180 lakes, some with ice covers that experience annual thawing such as Lake Stancionnoye (**A**) at Novolazarevskaya. Cryoconite assemblages at Schirmacher and Untersee range from massive boulders (**B**) to submillimeter accumulations within the ice (**C**). Classical analytical techniques include coring (**D**) to produce "hockey pucks" (**E**) for transport back home for laboratory analysis. Digital photographic techniques (**F**) offer the possibility of detecting microbial life *in situ* via fluorescent signatures from photosynthetic pigments elicited by laser excitation at 532 nm (**G**). The technique can also be used on site for more sensitive darkroom imaging of both the infrared fluorescence (**H**) and red-band fluorescence signatures (**I**). Color images available online at www.liebertonline.com/ast.

commonly been attributed to phycoerythrin, whose chromophores absorb light between 480 and 560 nm and produce fluorescence with peak values between 560 and 580 nm. In cyanobacteria, the light-harvesting unit is a hexameric protein aggregate sometimes associated with either of two chromophores: phycoerythrobilin (PEB) with optimal absorption between 550 and 565 nm, and phycourobilin (PUB) with an absorption optimum of 495 nm. PEB is required for energy transfer between units of the light-harvesting antenna and occurs in all phycoerythrin-containing marine cyanobacteria. Some strains of cyanobacteria, including strains of the ecologically important marine *Synechococcus* (Ong and Glazer, 1991), have PUB substituted for PEB to allow greater blue-green light absorption. Phycoerythrin spectral absorption peaks near 565 nm when only PEB chromophores are present. PUB chromophores shift the phycoerythrin absorption spectrum to 550–555 nm, and the fluorescence maximum shifts from 580 to 565 nm. Ocean phytoplankton fluorescence in the yellow band (580 nm) was originally ascribed only to the general phycoerythrin pigment class. However, predictable shifts in fluorescence yield, such as those described above, now make it feasible to estimate nutrient availability, water clarity, and even species information from L.I.F.E. spectral signatures (Olson *et al.,* 1990).

While remote detection of L.I.F.E. signatures following 532 nm excitation is relatively common at this time for terrestrial aquatic monitoring and has even been used to map subtle shifts in aquatic biomass composition, no systematic *in situ* or remote-sensing attempt has been made to extract such information from the ice of Arctic, Antarctic, or Alpine lakes and glaciers.

Hypothesis and Objectives

If infall material incorporated into the near-surface ice in the form of cryoconite sediments is relatively rich in organic material (Anesio *et al.,* 2009) and microbial communities that include photosynthetic cyanobacteria (Priscu *et al.,* 1998; Psenner *et al.,* 1999; Sattler *et al.,* 2004), then the availability of sunlight to provide both the heat energy necessary to melt the ice surrounding the assemblage and the energy for photosynthesis would confer a significant selective advantage on embedded cyanobacteria. Subsequent growth in the short Antarctic growing season should produce cyanobacteria-dominated assemblages that could be detected within the first few centimeters of the surface with fluorescence emission following excitation at 532 nm. We tested this prediction as part of the Tawani 2008 Antarctic Expedition to Schirmacher Oasis and Lake Untersee, Dronning Maud Land, Antarctica (Fig. 1) during the months of November and December 2008.

Methods and Materials

Field test sites

Primary field tests sites were annually frozen lakes of the Dry Valleys of Schirmacher Oasis near the Russian support station of Novolazarevskaya (Figs. 1A and 2B) at 70°46′04″S and 11°49′54″E, and Lake Untersee (Fig. 5A, 5B), a perennially ice-covered lake at 71°20′S and 13°26′E. Novolazarevskaya is 80 km from the Lazarev Sea coast at the southeastern tip of the Schirmacher Oasis, a 17×3 km bedrock strip running from west-northwest to east-southeast. An ice shelf resting against an ice cap extends north of the station near Leningradsky Bay, while a continental ice sheet slope extends to the south. The majority of the approximately 180 lakes in the oasis maintain their ice cover in the summer, while the bedrock of the oasis is characterized by the absence of continuous ice cover in both summer and winter. Annual precipitation is between 250–300 mm, and relative air humidity is approximately 50%. On the basis of humidity, snowfall, and ice cover, the oasis is considered one of the Antarctic Dry Valleys of great utility as a Mars analog test site.

In 1939, pilots of the German Antarctic Expedition discovered Lake Untersee or simply Untersee (English translation: the "under lake") 90 kilometers inland from the Schirmacher Oasis along the northeastern borders of the Gruber mountain range (Ritscher, 1942). A 2.5 m ice shield has covered the largest freshwater lake in East Antarctica (Kosenko and Kolobov, 1970) since it arose from a meltwater pond during climatic optimum periods in the Holocene (Hermichen *et al.,* 1985). Ice ablation in the arid climate is estimated to be 300 mm per year, and Cl^- concentration data indicate that at one point in its evolution the lake contained more than 50 times the current amount of meltwater. Significant microbial methanogenesis occurs in the sediment of a meromictic basin in the southeastern end of Untersee (Wand *et al.,* 1997). Cryoconite assemblages for Untersee range from meter to micrometer scales (Figs. 2B, 5D–H).

Sample collection

Ice cores 7.25 cm in diameter were obtained with a hand-driven Kovacs® ice corer (Fig. 2D, 2E). Ice slabs were extracted with a McCormick chain saw. Cryoconite sediments were sampled with a sterilized spoon out of multiple cryoconite holes in the lake ice. Lake sediment was collected with a sediment corer (UWITEC) at a depth of 40 m.

Digital imaging

A Zeiss Axioplan epifluorescence microscope provided broadband incoherent illumination with excitation filters centered at 370, 438, 480, and 548 nm. Images were acquired with an Optotronics ZVS-47EC CCD camera and processed with the imageJ image analysis software. For *in situ* photography, digital ultraviolet (UV), visible, and near-infrared (NIR) fluorescence images were obtained with the Foveon Fx17-78-F13 CMOS sensor in a Sigma SD14 digital single lens reflex camera (Fig. 2F). The sensor exhibits stable quantum efficiencies of 25%, 55%, and 25% at 390, 520, and 800 nm, respectively, and generates true three-band color images without filters (Gilblom *et al.,* 2003) via differential light absorption in silicon. A silicon sensor absorbs different wavelengths of light at different depths with absorption efficiencies that vary by 2 orders of magnitude across visible wavelengths (Hytti, 2005). Foveon detectors use three layers of sensors embedded at 0.2, 0.8, and 3.0 μm depths in the silicon, so the first layer records blue, the second green, and the deepest layer records red photons. Photon energy discrimination is accomplished simply by the differential absorption in the silicon chip as a function of depth. Of particular importance for L.I.F.E. experiments is the observation that the three-dimensional layered sensor geometry

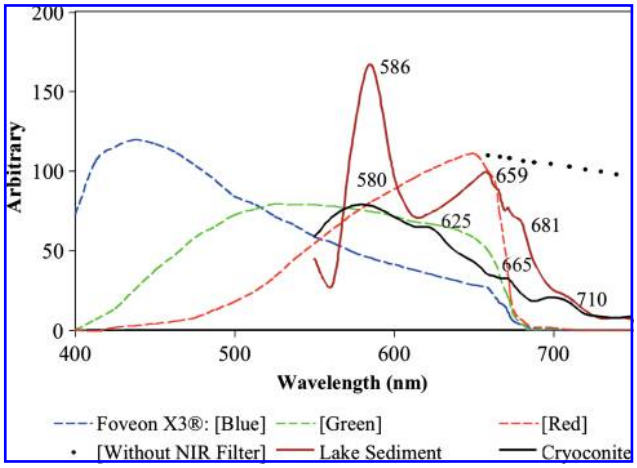

FIG. 3. Silicon response curves for red, green, and blue depict relative sensitivity of red and blue channels both with and without infrared blocking filter. Spectrum of the Untersee sediment exhibits peak responsivity at 586 and 659 nm compatible with attribution of the signal to phycoerythrin pigment. Shoulders at 681 and 710 nm may be indicative of other photosynthetic pigments. The spectral response predicts that the signal should appear in both RGB and IR modes. Signal strength for cryoconite shows optimal activity at 580 nm with shoulders appearing at 625, 665, and 710 nm.

makes it possible to combine information from the three layers to form a clean, sharp, virtually artifact-free luminance signal for each individual pixel (Hubel, 1999; Hubel *et al.*, 2004).

The camera also contains an easily removable infrared (IR) protective covering for the CMOS sensor. Removal of this IR-blocking filter and the addition of a Hoya R72 visible-light-blocking filter transform the system into an efficient NIR camera. Hoya O54, O56, and O58 high-pass filters can provide 95% blocking of laser excitation source but at the expense of a significant portion of the fluorescent response from phycoerythrin, some of which occurs in close proximity to the excitation wavelength. *In situ* experiments at the lake sites were performed without filters. Figure 3 depicts the relative spectral photon collection efficiency for the three sensor layers. These responses include the effects of 400 and 660 nm filters. The increase in performance in the NIR with removal of the protective IR filter is shown from 660 to 750 nm. For comparison, plots are included of the L.I.F.E. spectral signatures generated following 532 nm excitation of Untersee cryoconite sediment and lake bottom sediment collected from beneath a red cyanobacteria mat. The fine structure of these spectra will be discussed below. Red and green band response should be significantly more efficient than blue band for the spectra activity maxima at 570 nm for the cryoconite and 586 nm for the lake sediment. The red band should be well suited for the lake sediment activity at 659 nm. Lake sediment spectrum shoulders at 681 and 710 nm, and cryoconite activity at 705 nm will be best acquired by the Foveon chip in the NIR.

Data collection was performed in a darkroom (Fig. 2H), in open daylight (Fig. 2C, 2E, 2F) and in daylight scattering through lateral ice but with direct sunlight blocked by a photography cloak (Figs. 5C–H). Signal processing was performed with the Os X version of NIH Image, imageJ. Data were initially acquired in RAW format, converted to TIFF files without compression, and split into blue, green, and red channels for deconvolution and extraction of the fluorescence response. Analysis of a co-registered Speculon® standard made possible the digital removal of bleed-through reflected laser line contamination by calculating expected differences in blue and red band as a function of green band response for each pixel on the standard when illuminated with 532 nm light. Figure 4 depicts the red-band Speculon® response as a function of blue-band intensity for the region of maximum laser excitation, that is, where green-channel grayscale (gs) levels are saturated with [gs] = 255. The expected red-band response is well behaved and can be fitted with a third-order polynomial. Final differences between R and B for each pixel were corrected for expected differences prior to generation of the fluorescence image data shown in Figs. 6, 7, and 8, and determination of the final L.I.F.E. signature, $F_{[r-b]}$. UV-visible-NIR spectral data from 200 to 850 nm were obtained via an Ocean Optics USB 2000® fiber-optic spectrometer to document the probable source of the fluorescence response.

Laser excitation

Target excitation was accomplished with multiple 532 nm Class IIA lasers with 5 mW output power. These devices are powered by two AAA (1.5 V) lithium batteries, measure 16.2 cm in length, and weigh 85 gm. For *in situ* excitation of miniature cryoconites in the lake surface ice, the laser D86 beam diameter at target distance of 20 cm was

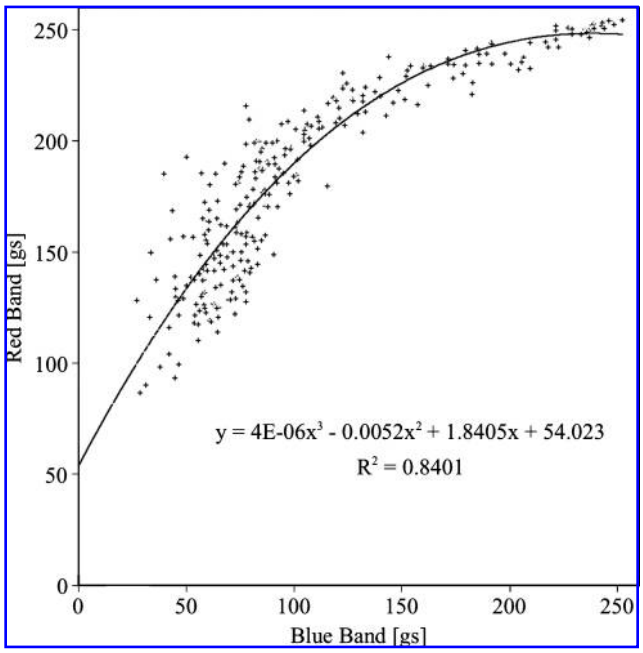

FIG. 4. Response for Foveon sensor red channels as a function of blue-band intensity for regions of the image exhibiting green-channel saturation from 532 nm laser light can be predicted with use of a third-order polynomial. The algorithm allows image deconvolution, removal of reflectance contamination, and reconstruction of embedded fluorescence response.

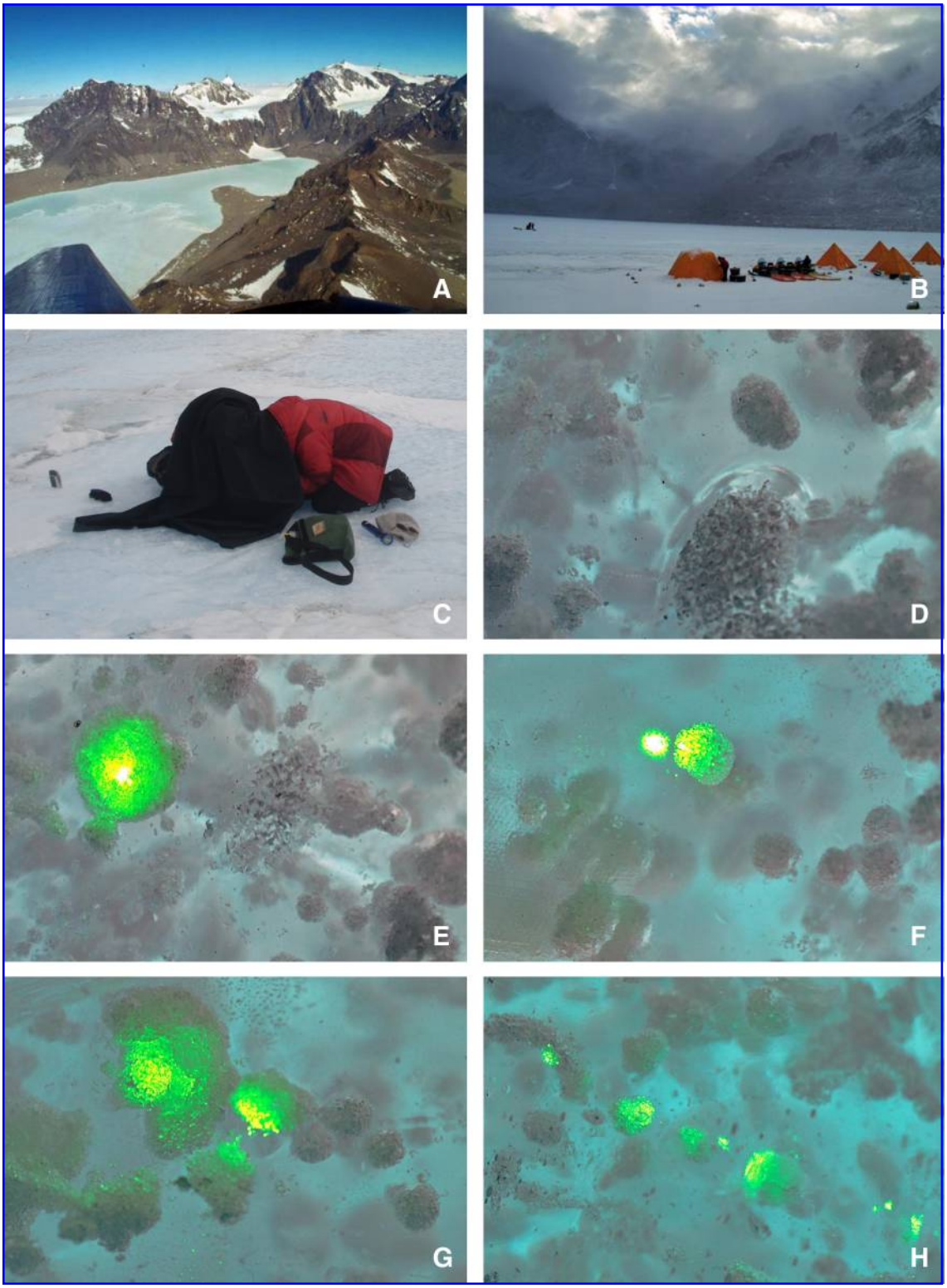

FIG. 5. Approaching the Anuchin Glacier and Untersee in a modified DC-3 Basilar transport provides an unobstructed view (**A**) of the field site from an altitude of 500 meters. Base camp (**B**) on the north edge of the central peninsula jutting into the lake provided ready access for *in situ* and sampling efforts. *In situ* imaging was accomplished both in open sunlight and under a blackened photographic hood (**C**). Assemblages of humic material and microorganisms forming the core of the miniature cryoconite worlds (**D**) were easily imaged with a 532 nm laser (**E**–**H**). Signal from the primary laser contact was enhanced by secondary reflections to neighboring cryoconites. Color images available online at www.liebertonline.com/ast.

$\sim 2.7 \pm 0.1$ mm. For illumination of larger sediment samples, the beam was expanded to 5.0 ± 0.2 mm with a compound Leitz objective lens. Total radiation exposures for 532 nm laser ranged from 1 to 10 mJ.

Results

Near-infrared versus visible wavelength imaging

Initial testing of the L.I.F.E. imaging techniques was completed in November 2008 during early Antarctic spring in the Schirmacher Oasis at Lake Stancionnoye near the Russian support station at Novolazarevskaya (Fig. 2A). The lake exhibits significant accumulation of miniature cryoconite assemblages (Fig. 2C, 2E, 2G) across the entire lake surface. Core samples were taken (Fig. 2D, 2E), and L.I.F.E. images were obtained both *in situ* (Fig. 2F, 2G) and in a dark room (Fig. 2H, 2I). Figure 2H depicts the NIR fluorescence image of one such core following excitation at 532 nm. The NIR fluorescence emphasizes the response from distributed micrometer-scale dust embedded in the core and highlights cryoconite accumulations in cracks and larger inclusions. The image depicted in Fig. 2I is the [r–b] visible wavelength fluorescence response to 532 nm excitation. The image includes removal of all nonlinear components of the raw image as outlined in Methods and Materials. The shorter-wavelength light provides higher resolution of cryoconite assemblages. While the NIR response was quite strong in a protected darkroom setting, *in situ* work was compromised by significant background scattering. The remaining *in situ* experiments were accomplished at visible wavelengths.

Cryoconite structure

The next set of experiments was conducted *in situ* at Lake Untersee (Fig. 5A, 5B). Reflected light red-green-blue (RGB) images obtained with partial shielding from diffuse solar radiation (Fig. 5C) easily revealed the accumulations of dust embedded within lake miniature cryoconite assemblages in the first 5 cm of ice (Fig. 5D). The structure of these ecosystems is evident in the image of the assemblage captured in the lower center of Fig. 5D. The core ellipsoidal aggregation of cryoconite material is surrounded by a smooth change in refractive index, which is most likely the result of a localized phase shift from ice to a mixture of liquid water and absorbed surface air, with or without oxygen generated by resident photosynthetic microorganisms.

Laser optical characteristics in transparent ice

At high laser intensities, the excitation beam produces one of three results: illumination of the prime target only (Fig. 5E), prime target illumination plus reflected illumination of one or more targets lateral to the original laser path (Fig. 5F, 5G), or penetration of the prime and multiple deeper targets along the original laser light path (Fig. 5H).

Discrimination of fluorescence sources

Figure 6 depicts the visible light response (Fig. 6A) and the fluorescence response (Fig. 6B) of a single cryoconite sphere illuminated *in situ* with 532 nm laser light. Relative 3-D light cones of fluorescent response (Fig. 6C) and the computation of fluorescence response isobars (Fig. 6D) document that the

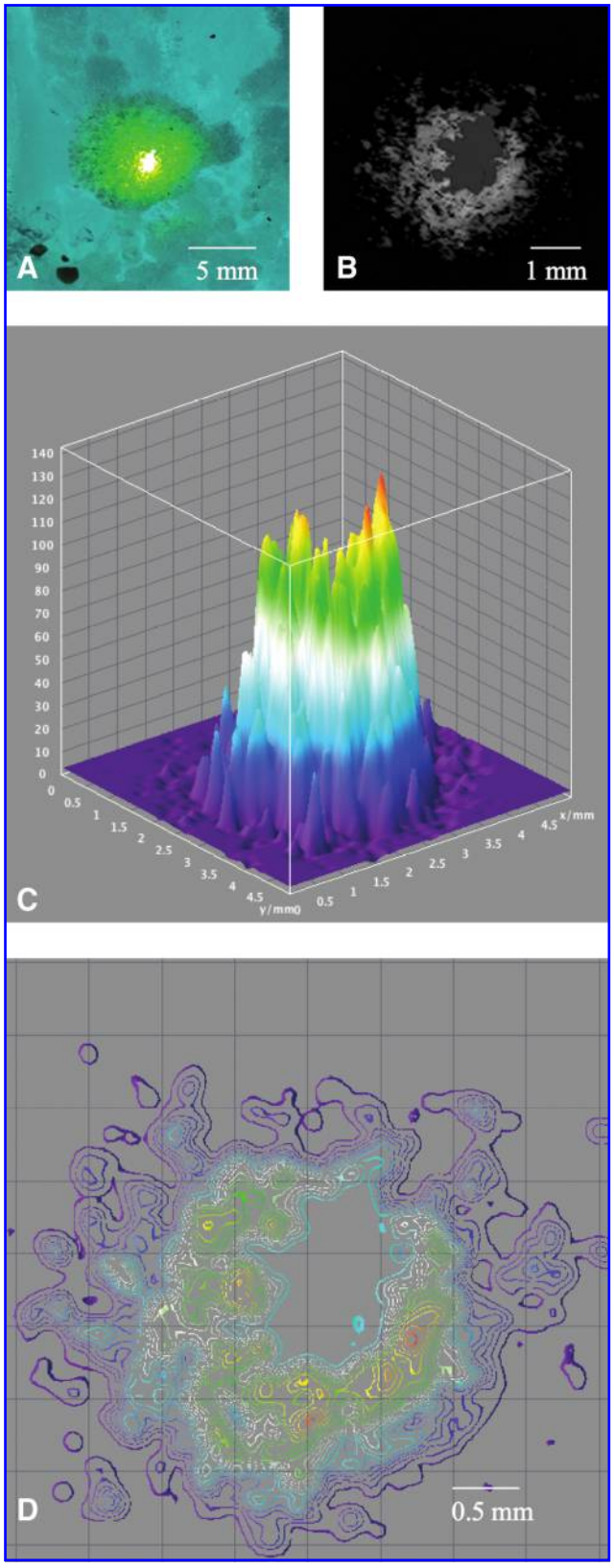

FIG. 6. A single cryoconite illuminated *in situ* with 532 nm laser light (**A**) produces a fluorescence response (**B**) in spatially discrete concentrations. Three-dimensional light distribution cones of fluorescent response and the isobar localization of source regions appear in (**C**) and (**D**), respectively. Color images available online at www.liebertonline.com/ast.

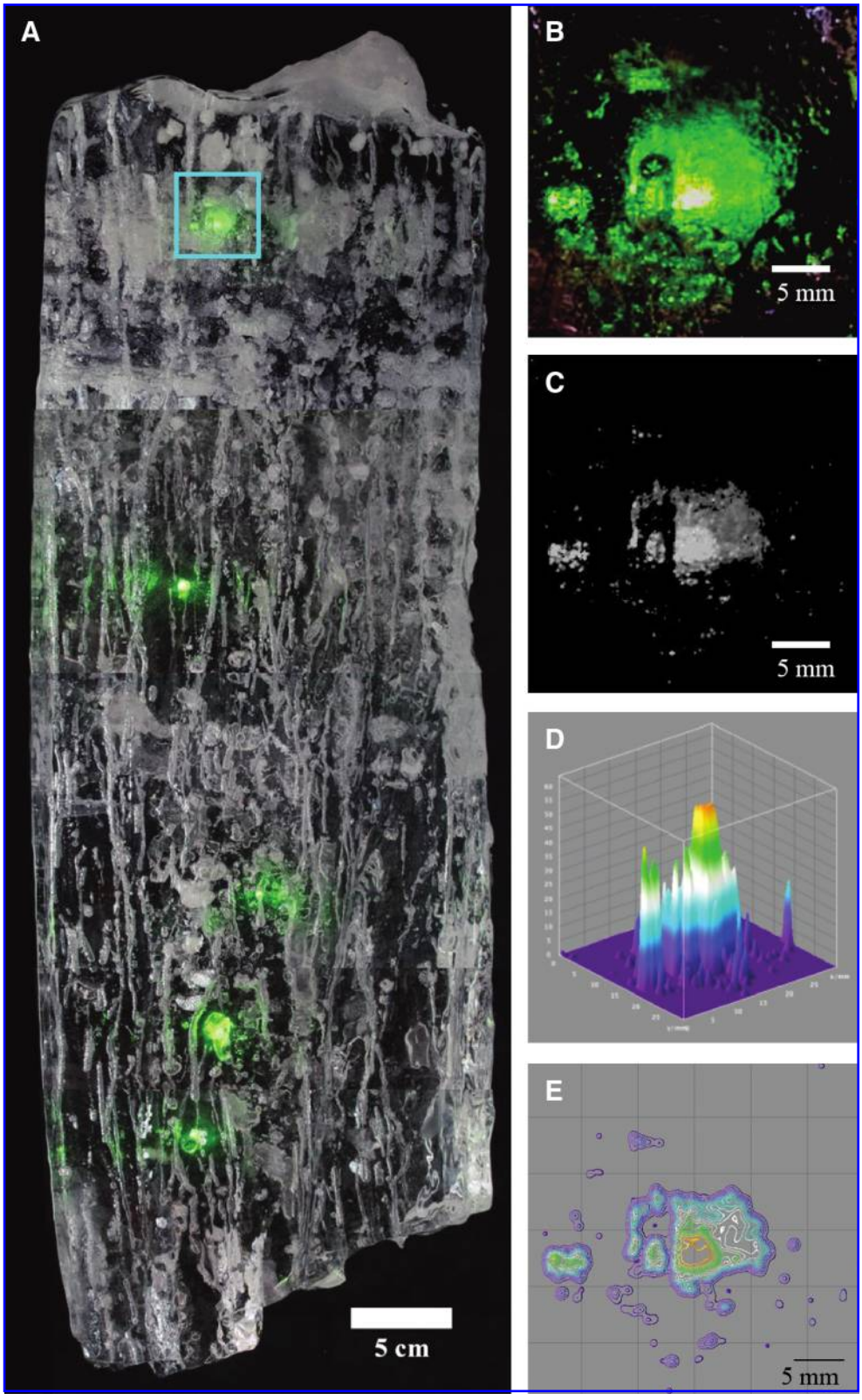

FIG. 7. A 65 cm rectangular slab of Untersee ice extracted from above the anoxic trough at the north end of Untersee (**A**) exhibits strong fluorescence response to 532 nm laser illumination of individual cryoconite targets at 6.4, 24.2, 39.2, 45.9, and 51.3 cm depth. Reflected light (**B**) and fluorescence (**C**) images plus light cone (**D**) and isobar (**E**) characterization of the target at 6.4 cm are depicted. The remaining four targets illustrated are depicted in Fig. 8. Construction of individual light cones (D) and isobars (E) makes it possible to spatially localize accumulations of putative photosynthetic communities. Target diameters range from less than 0.2 to 2.5 mm. (Ice slab sample courtesy of A. Mortvedt.) Color images available online at www.liebertonline.com/ast.

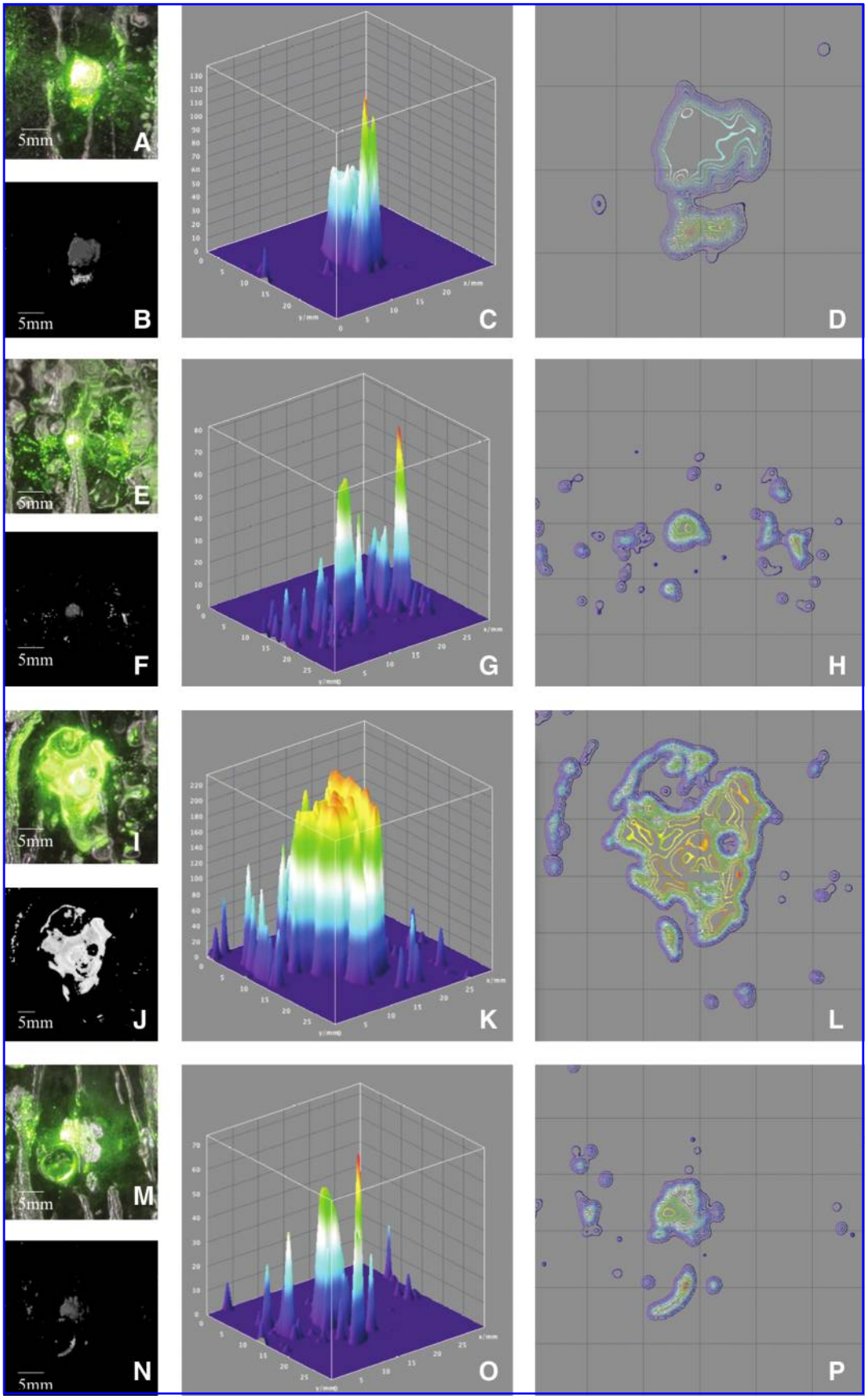

FIG. 8. Visible (**A–D**) and fluorescence (**E–H**) images and the light cone (**I–L**) and isobar (**M–P**) characteristics of cryoconite targets 24.2, 39.2, 45.9, and 51.3 cm below the surface of the Untersee ice covering document the discrete nature, location, and size of fluorescence sources. Color images available online at www.liebertonline.com/ast.

sources of fluorescence activity are discrete clusters of targets rather than a source which is diffusely spread throughout the cryoconite target. Source diameters for this sample range from 0.1 to 0.5 mm. Figures 7, 8, and 9 present the results of laser interrogation of five cryoconite assemblages surveyed in a 0.65 m slab of ice excised from the ice cover over the anoxic trough at the northeastern end of Untersee. Experiments were conducted within a partially blacked-out laboratory tent on the lakeshore, which was used for microscopic fluorescent imaging. Targets shown here were selected from depths of 6.4, 24.2, 39.2, 45.9, and 51.3 cm (Fig. 7A). A 3×3 cm RGB image of the first target appears in Fig. 7B. The $F_{[r-b]}$ deconvolved fluorescence signature appears in Fig. 7C. Analysis of the fluorescence light cones (Fig. 7D) and grayscale isobars (Fig. 7E) for the image revealed that the origin of the signature is again not homogeneous but comprised of clustered, discrete fluorescing sources similar to those depicted in Fig. 6 for cryoconites interrogated *in situ* from the lake surface. Figure 8 presents the reflectance and fluorescence signatures, along with the light-cone and isobar analysis of the remaining four cryoconites examined.

Figure 9 depicts the total fluorescence signal, $F_{[r-b]}$, for each of the five sites presented in Figs. 7 and 8. When working with optically thick targets such as soil or rock, the fluorescence response is confined to the area of primary laser excitation. As noted above in the laser optical path geometry observations, optically thin ice presents the possibility that ice-water or ice-gas phase-transition regions in the initial laser target might produce refraction events, reflection events, or both. The primary target now serves as a new laser excitation source. Consequently, $F_{[r-b]}$ was determined for both the 25 and 900 mm^2 areas around the primary laser excitation region. Local (25 mm^2) excitation accounts for only 26.5 ± 14.1% of the available signal. The total fluorescence

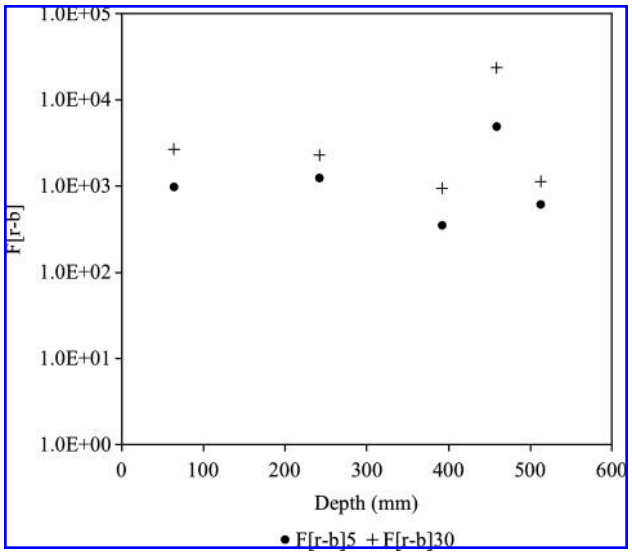

FIG. 9. Total fluorescence signal, $F_{[r-b]}$, for each of the five sites depicted in Figs. 7 and 8 was determined for 25 mm^2 and 900 mm^2 area around incident laser site. Local laser excitation (25 cm^2) accounts for only 26.5 ± 14.1% of the available signal. Fluorescence signal is relatively constant with depth except for the exceptionally active target at 45.9 cm.

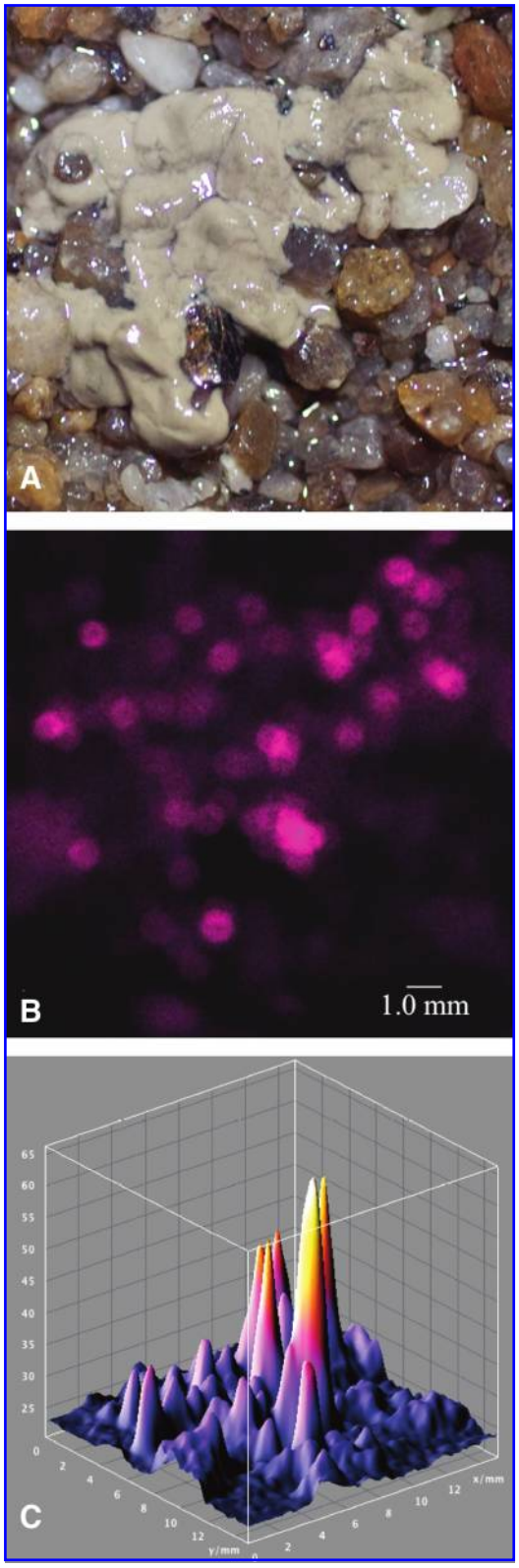

FIG. 10. Untersee sediment (**A**) extracted from below massive cyanobacterial mats produces infrared fluorescence signatures (**B**) following 532 nm excitation, and light cones (**C**) identify discrete spatial localization of sources. This sediment generated the spectral signature depicted in Fig. 3 attributed to phycoerythrin photopigments. Color images available online at www.liebertonline.com/ast.

signal is relatively constant for both collection areas except for the significantly more active target at 45.9 cm.

Untersee sediment and water

Untersee lake sediment (Fig. 10A) extracted from below a collection of red cyanobacteria mats produced infrared fluorescence signatures (Fig. 10B) following 532 nm excitation. Once again, light-cone characterization provides identification of discretely localized sources 1–2 mm in diameter. The 532 nm excitation of the sediment depicted in Fig. 10 generated the spectral signature in Fig. 3 attributed to phycoerythrin and other unidentified photopigments. Fluorescence activity at 586 and 659 nm is compatible with attribution of the signal to phycoerythrin. Shoulders at 681 and 710 nm may be indicative of other photosynthetic pigments. The significantly weaker signal from the cryoconite material collected from lake surface above the area of bottom sediment collection shows optimal activity at 580 nm, also attributable to phycoerythrin, but shoulders at 625, 665, and 710 nm may imply a more diverse set of photopigments. The spectral response predicts that the signal should appear in both RGB and IR modes but should be strongest in visible wavelengths. Figure 11 depicts the fluorescence response to 370 nm excitation (Fig. 1A) with use of a standard Zeiss Axioplan microscope for a cyanobacteria isolated from Untersee lake water. Figure 11B is a false-color image generated from the epifluorescence response to 438 nm (coded blue), 480 nm (green), and 548 nm (red).

Discussion and Conclusions

Earth may have been ice-covered for 10 million years or more on at least two occasions in a process known as "Snowball Earth" (Kirschvink *et al.,* 2000). During these periods of global glaciation, icy microbial ecosystems may have served as a refuge for photosynthetic life on the planet (Vincent and Howard-Williams, 2000; Priscu and Christner, 2004). The microbial communities that inhabit cryoconites must adapt and evolve in a similar hostile cryosphere and adapt to high UV radiation loads, freeze-thaw cycles, and organic resources dependent on limited photosynthetic primary production (Tranter *et al.,* 2004). As such, cryoconite assemblages and their icy habitat have been proposed as a model system for understanding the challenges microbial life would face on Earth or Mars early in the evolution of these planets (Horneck, 2000).

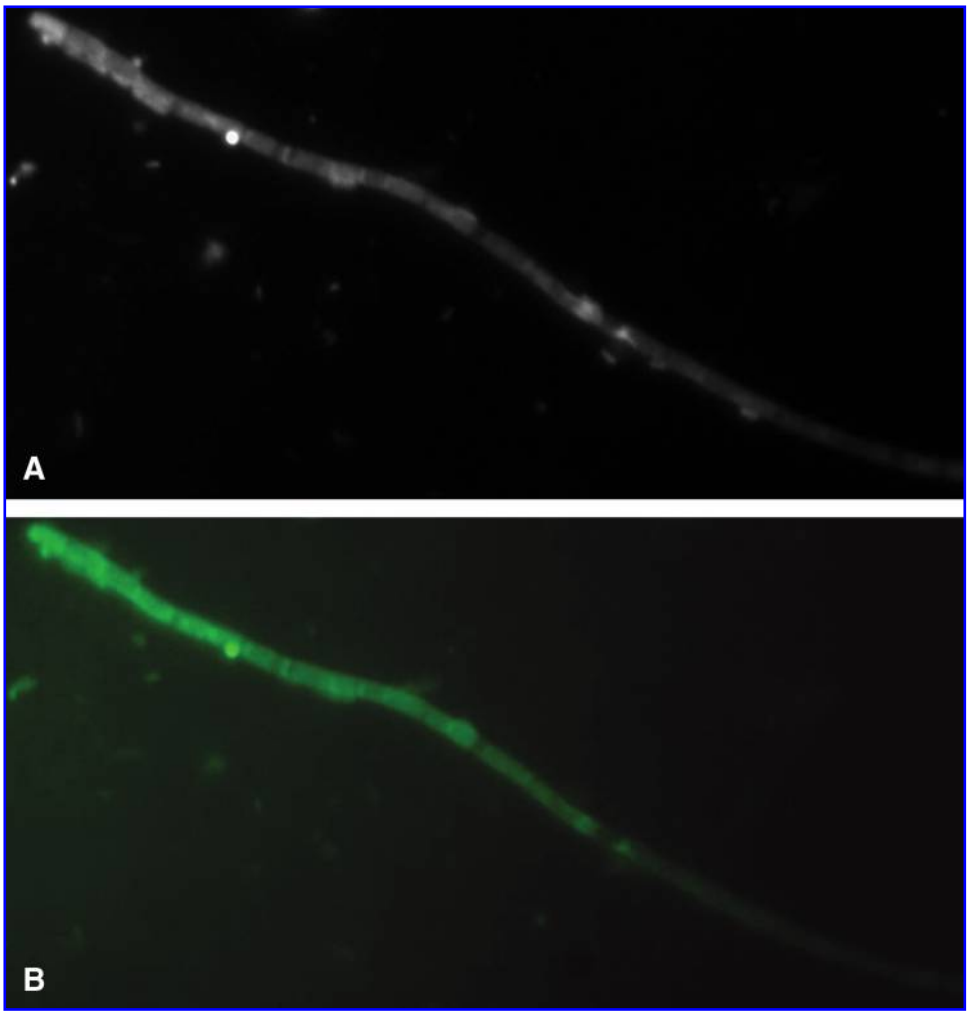

FIG. 11. Fluorescent image of cyanobacteria isolated from Untersee with excitation at 370 nm (**A**) and a falser-color image constructed from fluorescence images following excitation at 438 nm (blue), 480 nm (green), and 548 nm (red) (**B**).

Multiple efforts are currently underway to devise nondestructive *in situ* and remote detection technology to explore life in ice both on Earth and on other terrestrial planets. Many of these efforts are modifications of familiar laboratory techniques that are now beginning to prove useful and reliable in the field. Junge and coworkers have used optical and epifluorescence microscopy to delineate microbial habitats within ice veins (Junge *et al.,* 2004a, 2004b). Using F420 autofluorescence, Tung and colleagues demonstrated that microorganisms, including methanogens, can perform metabolic functions on clay grains 3 kilometers deep in the Greenland ice (Tung *et al.,* 2006). Particularly encouraging for Antarctic bioremediation monitoring is the recent development of a harmonic modulation technique that makes possible the use of UV light–emitting diodes for frequency-domain fluorescence lifetime probes capable of discriminating microbial life from diesel fuels (Zukauskas *et al.,* 2008).

The current work demonstrates that with minimal, inexpensive, off-the-shelf equipment it is feasible to generate laser-induced fluorescence imaging signatures for cryoconites in clear translucent Antarctic lake ice via a 532 nm laser diode. It should be noted that, while this is useful for detecting photosynthetic cyanobacteria containing phycoerytherin, these targets make up only a portion of the rich and diverse microbial population that inhabits Earth's cryosphere. Nor is 532 nm necessarily the optimal excitation wavelength for all species of cyanobacteria. Maximum absorption and subsequent optimal fluorescence response varies with cyanobacteria species and metabolic state but may occur anywhere between 400 and 550 nm with a secondary optimum between 650 and 700 nm (Schmidt and Trissl, 1998; Erokhina *et al.,* 2002; Polerecky *et al.,* 2009). With advances in laser diode construction during the past 3 years it is now possible to employ 375, 405, 437, 532, and 660 nm sources to probe NADH, FAD, and carotinoids as well as the chlorophylls and phycobilirubins. However, detection of a fluorescence following either broadband solar or laser excitation is a phenomenon that requires a clear optical path for both excitation and emission photons. As such these are near-surface probes that will require future ground-truth studies to understand depth constraints for snow, lake ice, and sea ice targets. It should also be noted that, while it is possible for a laser to produce target damage at any wavelength, it is much less probable for these longer wavelengths, particularly at 532 nm (Voskanyan, 1990, 1999), than is the case for deep UV (200–250 nm) probes (Fendrihan *et al.,* 2009). In this study, radiation exposure at 532 nm was >2 orders of magnitude below documented mutagenic or LD_{50} data documented to date.

The cryosphere covers *ca.* 10% of Earth's landmass, and up to 33 million square kilometers of the polar oceans are covered with seasonal or perennial ice. Active microbial communities in the ice play a central role in determining the availability of newly produced and released organic carbon that supports higher forms of life and are now known as important suppliers of usable organic carbon (Anesio *et al.,* 2009). Developing a multiwavelength laser imaging survey tool for aircraft or orbital platforms that targets different pigments would make it possible to monitor the carbon load of Earth's cryosphere and remotely search for life in the icy polar regions of Mars or terrestrial exoplanets.

Acknowledgments

The authors gratefully thank the Tawani Foundation, the Austrian Ministry of Science and Research, and the Kinohi Institute for financial and logistical support required for this study. We thank each of the members of the Tawani 2008 Antarctic Expedition for their comments, encouragement, and physical help on site. We particularly thank R. Psenner for useful discussions and A. Mortvedt, the expedition leader, for repeated assistance in acquiring difficult samples. B.S. was funded by the Austrian Academy of Sciences, Planetary Studies Foundation, and the Tyrolean Science Fund.

Abbreviations

IR, infrared; L.I.F.E., laser-induced fluorescence emission; NIR, near infrared; PEB, phycoerythrobilin; PUB, phycourobilin; RGB, red-green-blue; UV, ultraviolet.

References

Anesio, A.M., Hodson, A.J., Fritz, A., Psenner, R. and Sattler, B. (2009) High microbial activity on glaciers: importance to the global carbon cycle. *Glob. Chang. Biol.* 15:955–960.

Asher, S.A. (1993) UV resonance Raman spectroscopy for analytical, physical, and biophysical chemistry. 1. *Anal. Chem.* 65:A59–66.

Bhartia, R., Hug, W.F., Salas, E.C., Reid, R.D., Sijapati, K.K., Tsapin, A., Abbey, W., Nealson, K.H., Lane, A.L., and Conrad, P.G. (2008) Classification of organic and biological materials with deep ultraviolet excitation. *Appl. Spectrosc.* 62: 1070–1077.

Blinks, L.R. (1954) The photosynthetic function of pigments other than chlorophyll. *Annu. Rev. Plant Physiol.* 5:93–114.

Erokhina, L.G., Shatilovich, A.V., Kaminskaya, O.P., and Gilichinskii, D.A. (2002) The absorption and fluorescence spectra of the cyanobacterial phycobionts of cryptoendolithic lichens in the high-polar regions of Antarctica. *Microbiology* 71:601–607.

Fendrihan, S., Bérces, A., Lammer, H., Musso, M., Rontó, G., Polacsek, T.K., Holzinger, A., Kolb, C., and Stan-Lotter, H. (2009) Investigating the effects of simulated martian ultraviolet radiation on *Halococcus dombrowskii* and other extremely halophilic Archaebacteria. *Astrobiology* 9:104–112.

Fisk, M.R., Storrie-Lombardi, M.C., Douglas, S., McDonald, G.D., and Popa, R. (2003) Evidence of biological activity in Hawaiian subsurface basalts. *Geochemistry, Geophysics, Geosystems* 4:1–24.

Foreman, C.M., Sattler, B., Mikucki, J.A., Porazinska, D.L., and Priscu, J.C. (2007) Metabolic activity and diversity of cryoconites in the Taylor Valley, Antarctica. *J. Geophys. Res.* 112, doi:10.1029/2006JG000358.

Gilblom, D.L., Yoo, S.K., and Ventura, P. (2003) Operation and performance of a color image sensor with layered photodiodes. *Proceedings of SPIE* 5074:318–331.

Griffiths, A.D., Coates, A.J., Muller, J.-P., Storrie-Lombardi, M., Jaumann, R., Josset, J.-L., Paar, G., and Barnes, D. (2008) Enhancing the effectiveness of the ExoMars PanCam instrument for astrobiology. *Geophysical Research Abstracts* 10:EGU2008-A-09486.

Hermichen, W.-D., Kowski, P., and Wand, U. (1985) Lake Untersee—the first isotope study of the largest fresh-water lake in the interior of East Antarctica. *Nature* 315:131–133.

Hodson, A.J., Mumford, P.N., Kohler, J., and Wynn, P.M. (2005) The High Arctic glacial ecosystem: new insights from nutrient budgets. *Biogeochemistry* 72:67–86.

Hodson, A.J., Anesio, A.M., Tranter, M., Fountain, A.G., Osborn, M., Priscu, J., Laybourn-Parry, J., and Sattler, B. (2008) Glacial ecosystems. *Ecol. Monogr.* 78:41–67.

Hoge, F.E. and Swift, R.N. (1981) Airborne simultaneous spectroscopic detection of laser-induced water Raman backscatter and fluorescence from chlorophyll *a* and other naturally occurring pigments. *Appl. Opt.* 20:3197–3205.

Horneck, G. (2000) The microbial world and the case for Mars. *Planet. Space Sci.* 48:1053–1063.

Hubel, P.M. (1999) Image Color Image Quality in Digital Cameras. In *PICS 1999: Image Processing, Image Quality, Image Capture, Systems Conference,* The Society for Imaging Science and Technology, Springfield, VA, pp 153–157.

Hubel, P.M., Liu, J., and Guttosch, R.J. (2004) Spatial frequency response of color image sensors: Bayer color filters and Foveon X3. *Proceedings of SPIE* 5301:402–407.

Hytti, H.T. (2005) Characterization of digital image noise properties based on RAW data. *Proceedings of SPIE* 6059:A1–A13.

Junge, K., Eicken, H., and Deming, J.W. (2004a) Bacterial activity at −2 to −20°C in Arctic wintertime sea ice. *Appl. Environ. Microbiol.* 70:550–557.

Junge, K., Deming, J.W., and Eicken, H. (2004b) A microscopic approach to investigate bacteria under *in situ* conditions in Arctic lake ice: initial comparisons to sea ice. In *Bioastronomy 2002: Life Among the Stars, Proceedings of IAU Symposium #213,* edited by R. Norris and F. Stootman, Astronomical Society of the Pacific, San Francisco, pp 381–388.

Kirschvink, J.L., Gaidos, E.J., Bertani, L.E., Beukes, N.J., Gutzmer, J., Maepa, L.N., and Steinberger, R.E. (2000) Paleoproterozoic Snowball Earth: extreme climatic and geochemical global change and its biological consequences. *Proc. Natl. Acad. Sci. U.S.A.* 97:1400–1405.

Kosenko, N.G. and Kolobov, D.D. (1970) Obsledonanie ozera Unter-Zee [Observation of Lake Untersee]. In Russian. *Informat. Byull. Sov. Antarks. Eksped.* 79:65–69.

Lahav, O., Naim, A., Buta, R.J., Corwin, H.G., de Vaucouleurs, G., Dressler, A., Huchra, J.P., van den Bergh, S., Raychaudhury, S., Sodre, L., Jr., and Storrie-Lombardi, M.C. (1995) Galaxies, human eyes and artificial neural networks. *Science* 267:859–861.

Miteva, V. (2008) Bacteria in snow and glacier ice. In *Psychrophiles: from Biodiversity to Biotechnology,* edited by R. Margesin, F. Schinner, J.-C. Marx, and C. Gerday, Springer-Verlag, Berlin, pp 31–50.

Nealson, K.H., Tsapin, A., and Storrie-Lombardi, M. (2002) Searching for life in the universe: unconventional methods for an unconventional problem. *Int. Microbiol.* 5:223–230.

Olson, R.J., Chisholm, S.W., Zettler, E.R., and Armbrust, E.V. (1990) Pigments, size, and distribution of *Synechococcus* in the North Atlantic and Pacific Oceans. *Limnol. Oceanogr.* 35:45–58.

Ong, L.J. and Glazer, A.N. (1991) Phycoerythrins of marine unicellular cyanobacteria. I. Bilin types and locations and energy transfer pathways in *Synechococcus* spp. phycoerythrins. *J. Biol. Chem.* 266:9515–9527.

Polerecky, L., Bissett, A., Al-Najjar, M., Faerber, P., Osmers, H., Suci, P.A., Stoodley, P., and de Beer, D. (2009) Modular spectral imaging system for discrimination of pigments in cells and microbial communities. *Appl. Environ. Microbiol.* 75:758–771.

Porazinska, D.L., Fountain, A.G., Nylen, T.H., Tranter, M., Virginia, R.A., and Wall, D.H. (2004) The biodiversity and biogeochemistry of cryoconite holes from McMurdo Dry Valley glaciers, Antarctica. *Arct. Antarct. Alp. Res.* 36:84–91.

Price, P.B. (2007) Microbial life in glacial ice and implications for a cold origin of life. *FEMS Microbiol. Ecol.* 59:217–231.

Priscu, J.C. and Christner, B.C. (2004) Earth's icy biosphere. In *Microbial Diversity and Bioprospecting,* edited by A.T. Bull., ASM Press, Washington DC, pp 130–145.

Priscu, J.C., Fritsen, C.H., Adams, E.E., Giovannoni, S.J., Paerl, H.W., McKay, C.P., Doran, P.T., Gordon, D.A., Lanoil, B.D., and Pinckney, J.L. (1998) Perennial Antarctic lake ice: an oasis for life in a polar desert. *Science* 280:2095–2098.

Psenner, R. (1999) Living in a dusty world: airborne dust as a key factor for alpine lakes. *Water Air Soil Pollut.* 112:217–227.

Psenner, R. and Sattler, B. (1998) Life at the freezing point. *Science* 280:2073–2074.

Psenner, R., Sattler, B., Willie, A., Fritsen, C.H., Priscu, J.C., Felip, M., and Catalan, J. (1999) Lake ice microbial communities in Alpine and Antarctic lakes. In *Cold-Adapted Organisms: Ecology, Physiology, Enzymology and Molecular Biology,* edited by R. Margesin and F. Schinner, Springer-Verlag, Berlin, pp 17–31.

Ritscher, A. (1942) *Wissenschaftliche und fliegerische Ergebnisse der Deutschen Antarktischen Expedition 1938/39,* Vol. 1, Leipzig.

Rohde, R.A., Price, P.B., Bay, R.C., and Bramall, N.E. (2008) *In situ* microbial metabolism as a cause of gas anomalies in ice. *Proc. Natl. Acad. Sci. U.S.A.* 105:8667–8672.

Samsonoff, W.A. and MacColl, R. (2001) Biliproteins and phycobilisomes from cyanobacteria and red algae at the extremes of habitat. *Arch. Microbiol.* 176:400–405.

Sattler, B., Puxbaum, H., and Psenner, R. (2001) Bacterial growth in supercooled cloud droplets. *Geophys. Res. Lett.* 28:239–242.

Sattler, B., Waldhuber, S., Fischer, H., Semmler, H., Sipiera, P., and Psenner, R. (2004) Microbial activity and phylogeny in ice cores retrieved from Lake Paula, a newly detected freshwater lake in Antarctica. *Proceedings of SPIE* 5555:170–179.

Säwström, C., Mumford, P., Marshall, W., Hodson, A., and Laybourn-Parry, J. (2002) The microbial communities and primary productivity of cryoconite holes in an Arctic glacier (Svalbard 79°N). *Polar Biol.* 25:591–596.

Schmidt, K.A. and Trissl, H.-W. (1998) Combined fluorescence and photovoltage studies on chlorosome containing bacteria. II. Whole cells and chlorosome-depleted membranes of *Chlorobium limicola*. *Photosyn. Res.* 58:57–60.

Storrie-Lombardi, M.C. (2005) Post-Bayesian strategies to optimize astrobiology instrument suites: lessons from Antarctica and the Pilbara. *Proceedings of SPIE* 5906:288–301.

Storrie-Lombardi, M.C., Lahav, O., Sodre, L., and Storrie-Lombardi, L.J. (1992) Morphological classification of galaxies by artificial neural networks. *Mon. Not. R. Astron. Soc.* 259:8–12.

Storrie-Lombardi, M.C., Hug, W.F., McDonald, G.D., Tsapin, A.I., and Nealson, K.H. (2001) Hollow cathode ion lasers for deep ultraviolet Raman spectroscopy and fluorescence imaging. *Rev. Sci. Instrum.* 72:4452–4459.

Storrie-Lombardi, M.C., Muller, J.-P., Fisk, M.R., Griffiths, A.D., and Coates, A.J. (2008a) Potential for non-destructive astrochemistry using the ExoMars PanCam. *Geophys. Res. Lett.* 35, doi 10.1029/2008GL034296.

Storrie-Lombardi, M.C., Muller, J.-P., Fisk, M.R., Griffiths, A.D., and Coates, A.J. (2008b) Epifluorescence surveys of extreme environments using PanCam imaging systems: Antarctica and the Mars regolith. *Proceedings of SPIE* 7097:1–10.

Takeuchi, N. and Li, Z. (2008) Characteristics of surface dust on Ürümqi glacier No. 1 in the Tien Shan mountains, China. *Arct. Antarct. Alp. Res.* 40:744–750.

Takeuchi, N., Kohshima, S., and Seko, K. (2001) Structure, formation, and darkening process of albedo-reducing

material (cryoconite) on a Himalayan glacier: a granular algal mat growing on the glacier. *Arct. Antarct. Alp. Res.* 33:115–122.

Tranter, M., Fountain, A., Fritsen, C., Lyons, B., Statham, P., and Welch, K. (2004) Extreme hydrochemical conditions in natural microcosms entombed within Antarctic ice. *Hydrological Processes* 18: 379–387.

Tung, H.C., Price, P.B., Bramall, N.E., and Vrdoljak, G. (2006) Microorganisms metabolizing on clay grains in 3-km-deep Greenland basal ice. *Astrobiology* 6:69–86.

Vincent, W.F. and Howard-Williams, C. (2000) Life on Snowball Earth. *Science* 287:2421.

Voskanyan, K.S. (1990) 633 nm light induces mutations. *Studia Biophysica* 139:43–46.

Voskanyan, K.S. (1999) UV and visible light–induced mutations in *Escherichia coli*. In *Second Internet Conference on Photochemistry and Photobiology*. Available online at http://www.photobiology.com/photobiology99/contrib/karin/index.html.

Wand, U., Schwarz, G., Brüggemann, E., and Bräuer, K. (1997) Evidence for physical and chemical stratification in Lake Untersee (central Dronning Maud Land, East Antarctica). *Antarct. Sci.* 9:43–45.

Zukauskas, A., Vitta, P., Kurilcik, N., and Jursenas, S.E. (2008) Characterization of biological materials by frequency-domain fluorescence lifetime measurements using ultraviolet light-emitting diodes. *Optical Materials* 30:800–805.

Address correspondence to:
Michael C. Storrie-Lombardi
Kinohi Institute
1700 Alta Wood Drive
Pasadena, CA 91101
USA

E-mail: mike@kinohi.org